Arabian Journal of Chemistry (2020) 13, 8060–8068

King Saud University

Arabian Journal of Chemistry

www.ksu.edu.sa
www.sciencedirect.com

ORIGINAL ARTICLE

Attenuating effect of Indole-3-Carbinol on gold nanoparticle induced hepatotoxicity in rats

Maha Ibrahim Alkhalaf

Biochemistry Department, Faculty of Science- University of Jeddah, 21589, P.O. box 80200, Jeddah, Saudi Arabia

Received 30 June 2020; accepted 21 September 2020
Available online 1 October 2020

KEYWORDS

Gold nanoparticles;
Indole-3-carbinol;
Liver toxicity;
Antioxidants;
Oxidative stress;
Inflammation

Abstract Indole-3-carbinol (I3C) is a plant based compound present in vegetables mostly belonging to cruciferous family. I3C has been shown to possess anticancer, antioxidant and anti-inflammatory properties. Humans are increasingly being exposed to GNPs due an due to their widespread and increased applications in different fields. Consistently, recent animal and cell based studies have found them to be carcinogenic, prooxidant and inflammatory. This study sought to examine the beneficial effects of I3C against oxidative stress, inflammation and histopathological changes in liver tissues of rats administered with GNPs. Forty rats randomly divided into four groups: G1 control G2, rats injected i.p. with a suspension of GNPs (10 nm in size) (20 μg/kg body wgt) for 7 days; G3, rats supplemented orally with I3C (150 mg/kg body wgt) for 7 days; and G4, rats injected with GNPs along with oral supplementation ofI3C. Compared to control, rats administered with GNPs had significantly increased liver functional markers including ALT, AST, ALP, total and direct bilirubin and significantly decreased albumin levels. GNP administered rats also demonstrated increased oxidative stress and inflammatory markers, MDA, 8-OHdG and IL-6 levels and significantly depleted activities of antioxidants such as glutathione reductase (GR) and glutathione S-transferase (GST), and transcription factor, Nrf2 compared to control. GNPs also exerted marked histological changes in liver tissues. Treatment with I3C significantly restored the GNP induced changes in the levels of all the studied parameters and also prevented pathological changes in liver tissues. Molecular docking studies confirm the interaction of I3C with hepatic cell surface receptor protein LT3 and thereby blocking GNPs from binding to I3C, confirming above experimental findings. Collectively, the data demonstrate the hepatoprotective effects of I3C against GNP-induced adverse effects on liver tissue. These protective effects of I3C appear to be mediated by its ability to downregulate oxidative stress and inflammation. Thus dietary intake of plant products rich in I3C may have beneficial health effects.

E-mail address: mialkhalaf@uj.edu.sa
Peer review under responsibility of King Saud University.

Production and hosting by Elsevier

1. Introduction

Nanotechnology is an emerging scientific filed with with diverse application (Shu and Tang, 2019). The unique properties of nanoparticles including flexibility in functionalisation,

https://doi.org/10.1016/j.arabjc.2020.09.035
1878-5352

biocompatibility, resistance to oxidation and high surface reactivity make them ideal candidates to use in drug delivery, imaging and other medical applications (BarathManiKanth et al., 2010, Khan et al., 2013).

Among various nanoparticles, the noble metal nanoparticles such as gold nanoparticles (GNPs) gained immense importance due to their catalytic, electronic, fluorescence, and biological potential (Huang et al., 2018). However, increased and widespread use has led to an increased risk of human exposure to these GNPs. The application of GNPs includes their use in plasmon-based labeling and imaging, optical and electrochemical sensing, and diagnostics. Gold nanoparticles may also be used in photothermal and radiofrequency-mediated thermal therapies as well as delivery vehicles for genetic materials, imaging agents, and drugs (Adewale et al., 2019). Consistently, recent studies have shown that exposure to GNPs elicited cytotoxic, inflammatory reactions (Oberdörster et al., 2005, Nel et al., 2006, Adewale et al.,2019). Importantly, smaller-sized GNPs were found to be more toxic as opposed to larger-sized GNPs due to their increased reactivity and surface area which impact their contact and binding with the cells (Nel et al., 2006, Oberdörster et al., 2005).

Long-term oral exposure studies revealed that, GNPs accumulate in the main organs such as the liver and lungs (Sung et al., 2012). Resident phagocytes, including liver Kupffer cells and macrophages and B cells in spleen, play a major role in the uptake and accumulation of GNPs in liver and spleen (Xue et al., 2012). Abdelhalim and Jarrar (2011) affirming that, bioaccumulation of GNPs in rat tissues, such as liver, kidney, heart and lung, depends on the particle size and duration of exposure.

The phytochemical indole-3-carbinol (I3C) is a breakdown product of glucosinolates, which are a diverse group of small molecules produced in the Cruciferae family, including *Brassica* vegetables, such as broccoli and cauliflower (Katz et al., 2015).

Epidemiological studies suggest that, a low risk of developing cancer is linked to high dietary intake of cruciferous vegetables and that, their protective properties may be partly attributable to their I3C content. The I3C has shown to exert immunomodulatory, anti-microbial and anti-inflammatory effects. Additionally, I3C has proven effective in lowering the risk of developing different types of cancer including mammary glands and liver (Kim and Park, 2018). Importantly, I3C is a highly unstable molecule and several studies have attributed its effects to its dimer products, such as 3–3′-diindolylme thane (DIM) (Anderton et al., 2004, Leibelt et al., 2003, Reed et al., 2006). Therefore, the positive effects of I3C may actually be mediated by its dimer products.

The molecular docking approach can be used to model the interaction between a small molecule and a protein at the atomic level, which allows us to characterize the behaviour of small molecules in the binding site of target proteins as well as to elucidate fundamental biochemical processes (Cross et al., 2009; Li et al., 2010). The docking process involves two basic steps: prediction of the ligand conformation as well as its position and orientation within these sites (usually referred to as pose) and assessment of the binding affinity. These two steps are related to sampling methods and scoring schemes, respectively, which will be discussed in the theory section. Knowing the location of the binding site before docking processes significantly increases the docking efficiency. In many cases, the binding site is indeed known before docking ligands into it. Also, one can obtain information about the sites by comparison of the target protein with a family of proteins sharing a similar function or with proteins co-crystallized with other ligands. In the absence of knowledge about the binding sites, cavity detection programs or online servers (Plewczynski et al., 2011; McConkey et al., 2002).

The objective of this study was to examine the effect of GNPs on liver function, oxidative stress, inflammation and tissue architecture in rat liver and to assess the potential of I3C to reverse these GNP induced effects. We measured the liver functional markers including aspartate transaminase (AST), alanine transaminase (ALT), and alkaline phosphatase (ALP), albumin and bilirubin. Malondialdehyde (MDA), glutathione reductase (GR), glutathione S-trnasferase (GST), and 8-hydroxy-2′ -deoxyguanosine (8-OHdG) were measured to assess oxidative stress, while IL-6 levels were determined to assess inflammation. The nuclear factor erythroid 2–related factor 2 (Nrf2) was measured to understand its role in the effects of I3C. Additionally, H&E staining was carried out to assess histopathological changes in live tissue. Molecular docking studies were carried out to verify the favourable effects of I3C.

2. Materials and methods

2.1. Chemicals

The GNPs with a molecular weight of 196.97 and a diameter of 10 nm were obtained from Sigma-Aldrich Company (USA). The GNPs were supplied as stabilised suspension in citrate buffer. I3C was purchased from Fair vital –Bioactive Vitalstoffe Company, Europe). As reported by the supplier, the concentration, optical density, wavelength and polydispersity index of GNPs are ~ 6.0E + 12 particles/mL, 1, 510–525 nm and < 0.2 respectively.

2.2. Animals

Forty male Sprague Dawley rats (150–180 g body weight) were randomly divided into four groups with 10 rats in each group and housed in plastic cages. Rats were acclimatized for 2 weeks to laboratory conditions prior to initiation of experiments. Rats were maintained on standard laboratory conditions and had access water and normal chow diet ad libitum. The study was approved by the Ethical Committee of King Fahad Medical Research Center. Jeddah, KSA. Approval number (177–19).

The details of different groups are given below.

Group 1 (C): Healthy control.
Group 2 (GNPs): Rats were injected intraperitoneally (i.p). with a suspension of GNPs with a dose of 20 μg/kg body weight, daily for 7 days following the procedure described by Abdelhalim and Moussa, (2013)and Siddiqi et al., (2012).
Group 3 (I3C): Healthy rats were dosed orally by gavage with I3C at 150 mg/kg body weight daily for 7 days; the dose of 150 mg/kg body weight was comparable to those used by other researchers (Okulicz et al.,2009).

Group 4 (GNPs + I3C): Rats were injected with GNPs as described in Group 2 followed by a daily oral supplementation of I3C as described in Group 3.

At the end of treatment duration, rats were euthanized by diethyl ether. Blood samples were collected from hepatic portal vein, serum was separated by centrifugation at 1200*g* for 15 min and stored at − 20 °C until used. Liver tissues were excised, washed in cold saline and used for biochemical and histological examinations.

2.3. Determination of liver functional markers

Serum levels of liver functional markers including AST, ALT, and ALP activities were determined by following the manufacturer's instructions (Bio-Diagnostic). Total and direct bilirubin and albumin were determined by following the methods described by supplier (BioVision, Milpitas, CA, USA).

2.4. Determination of oxidative stress and inflammatory biomarker in liver tissues

Liver tissues were homogenized in Tris HCl buffer (0.1 mol/L, pH 7.4) and the homogenate was centrifuged at 4000*g* for 30 min. The clear supernatant was separated and used for estimating MDA, GR, GSH, 8-OHdG, IL-6 and Nrf2. Malondialdehyde in tissue homogenates was determined as thiobarbituric acid reactive substances (TBARS) according to the method of Draper and Hadley (1990). Briefly, reaction mixture containing tissue homogenate, SDS, acetic acid and thiobarbituric acid (TBA) was heated in a boiling water bath for 1 h and 2.5 ml n-butanol was added and centrifuged at 2500g for 10 min. Absorbance of the organic layer was read at 532 nm. The MDA content was expressed as nmol/mg protein.

The activity of GST was determined according to manufacturer's guidelines (Cloud-Clone Corp. USA). Briefly, 1.35 ml reduced glutathione (GSH) solution, 0.15 ml 1-chloro-2,4-dinitrobenzene (CDNB), 1.4 ml phosphate buffer, and 0.1 ml tissue homogenate were incubated at 25 °C and the absorbance was measured at 340 nm every minute for a total of 3 readings. Enzyme activity was expressed as nmol/min/mg protein. Glutathione reductase (GR) activity was measured using commercially available kits following the procedure recommended by supplier (Cloud-Clone Corp. USA). Briefly, reaction mixture in 0.5 ml of 0.2 M potassium phosphate buffer containing 1 mM EDTA, 250 µl of 5,5′-Dithio-bis-(2-nitrobenzoic Acid) (DTNB), 125 µl distilled water, 50 µl of NADPH, and 25 µl of the tissue homogenate and 50 µl L-glutathione oxidized (GSSG). The absorbance was measured at 412 nm and the content of GR was expressed as nmol/min/mg protein.

8-hydroxydeoxyguanosine (8-OHdG) was estimated by ELISA based assay as described by manufacturer (Kamiya Biomedical Company, USA). Briefly, tissue homogenates and standards were added to wells and incubated for 2 h. at room temperature. Wells were thoroughly washed, incubated with HRP-conjugated monoclonal primary antibodies and incubated for 1 h. at room temperature. Wells were washed thoroughly and incubated with TMB substrate in the dark for 30 min. Absorbance was measured at 450 nm and the content of 8-OHdG was inferred from standard curve and expressed as nmol/mg protein.

The levels of inflammatory marker, IL-6 and transcription factor, Nrf2 were determined in liver tissues by ELISA based assay following the manufacturer's instructions (LifeSpan Biosciences, USA). Briefly, wells precoated with anti-IL6 or anti-Nrf2 antibodies were incubated with supernatants of tissue homogenates or standards for 2 h at room temperature. Wells were washed and incubated with respective biotin labelled antibodies for 1 h. at room temperature. Wells were washed and further incubated with avidin-HRP conjugated secondary antibodies for 1 h. at room temperature. Wells were washed and incubated with substrate TMB. The OD was measured at 450 nm and the content of IL-6 or Nrf2 was inferred from the standard curve and expressed as pg/mg protein.

2.5. H&E staining of liver tissue

Liver tissue specimens were fixed in 10% formalin solution, sectioned and deparaffinised. Sections were stained with H&E and evaluated for histological changes under light microscopy.

2.6. Docking studies (Molecular docking)

Auto docking tools 4.2 module was used to predict the binding of drug candidates to the known 3D structure of receptors. Gasteiger partial charges were added to the atoms in ligand (designed drug). Rotatable bonds were clarified, and non-polar hydrogen atoms were conjoined. Kollman united atom type charges and salvation indices were applied following the addition of fundamental hydrogen atoms (Zayed et al., 2018a, 2019). Van der Waals and electrostatic bindings were determined using distance-dependent dielectric functions and auto Dock parameter set respectively. Lamarckian genetic algorithm and Solis & Wets local search method were executed for simulative docking. (Dobbs and Hehre, 1987) Orientation, initial position and torsions of the ligand molecule were set.

2.7. Statistical analysis

The SPSS Statistical programme for Windows (Version 19, (SPSS Inc., Chicago, IL, USA) was used for data analysis. The significance of difference between various groups was measured by one-way ANOVA (LSD) test. Data were expressed as the mean ± SD. $p < 0.01$ was considered significant.

3. Results

3.1. Liver functional markers

Serum levels of liver functional markers in different treatment groups of rats are presented in Table 1. Compared to control, rats treated with GNPs had significantly elevated ALT, AST, ALP, total and direct bilirubin ($p < 0.01$) and significantly declined albumin levels ($p < 0.01$). Whereas, rats co-treated with GNPs and I3C exhibited a significant reduction ($p < 0.01$) in ALT, AST, ALP, total and direct bilirubin and a significant increase in albumin levels as compared to those

Table 1 The levels of liver functional markers in serum of control and treated rats.

Parameters	G1 (control)	G2 (GNPs)	G3 (I3C)	G4 (GNPs + I3C)
ALT (U/L)	19.8 ± 1.68	61.3 ± 3.52[a]	20.2 ± 1.56[a]	41.9 ± 3.6[b]
AST (U/L)	47.1 ± 3.17	110.3 ± 2.7[a]	49.1 ± 2.0[a]	66.5 ± 3.5[b]
ALP (U/L	39.6 ± 3.16	117.9 ± 2.84[a]	40.3 ± 2.94[a]	60.9 ± 8.19[b]
Total bilirubin (mg/dL)	0.49 ± 0.03	1.72 ± 0.1[a]	0.49 ± 0.03[a]	0.49 ± 0.03[b]
Direct bilirubin (mg/dL)	0.23 ± 0.011	1.13 ± 0.027[a]	0.23 ± 0.009[a]	0.25 ± 0.02[b]
Albumin (mg/dL)	7.0 ± 0.14	2.3 ± 0.14[a]	7.1 ± 0.34[a]	6.1 ± 0.21[b]

AST, aspartate transaminase ALT, alanine transaminase; ALP, alkaline phosphatase. [a]Compared to G1 group, [b]Compared to G2, [ab]$p < 0.01$. Data are presented as mean ± SD (N = 10).

in GNP treated rats (group 2) Additionally, no significant change was observed between control and I3C alone treated rats (group 3).

3.2. Oxidative stress markers

The levels of oxidative stress markers in the liver tissues of control and different treatment groups of rats provided in Table 2. The MDA and 8-OHdG were significantly elevated in GNPs treated rats as matched to those in control rats. In contrast, antioxidants including GST and GR levels were significantly ($p < 0.01$) declined in in rats treated with GNPs as compared to control group. Co-treatment of rats with GNPs and I3C led to a significant ($p < 0.01$) reduction in MDA and 8-OHdG, and a significant elevation in GST and GR levels, compared to those in GNPs treated rats. The levels of all the studied markers in I3C treated rats were identical to the levels found in control rats indicating that I3C treatment alone exerted no significant change on these markers.

3.3. IL-6 and Nrf2

The levels IL-6 and Nrf2 in the liver tissues of control and different treatment groups are shown in Figs. 1 and 2. Rats treated with GNPs demonstrated a significant increase in IL-6 ($p < 0.01$) and a significant decrease in Nrf2 levels ($p < 0.01$) as compared to control group. On the other hand, a significant reduction of IL-6 ($p < 0.01$) and a significant augmentation of Nrf2 levels ($p < 0.01$) were noticed in rats co-treated with GNPs and I3C. Interestingly, a significant increase was observed in IL-6 level in G3 rats as compared to those in control($p < 0.01$). In contrast the Nrf2 levels in rats treated only with I3C were equal to the levels found in control.

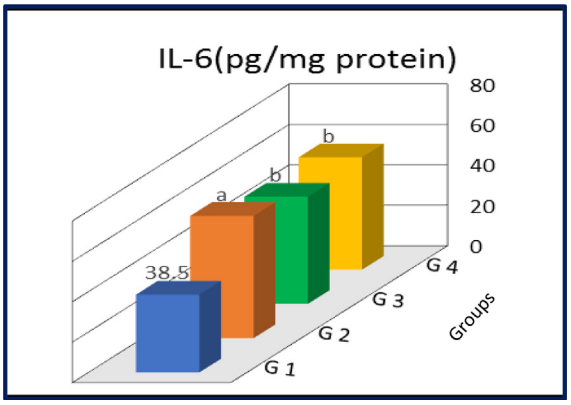

Fig. 1 IL-6 levels in liver tissues of control and treated rats. G1, control; G2, AuNP treated rats; G3, I3C treated rats; G4, AuNP + I3C treated rats. Data are presented as mean ± SD. [a]significantly different ($p < 0.01$) compared to G1 group [b]Significantly different ($p < 0.01$) compared to G2 group.

3.4. Liver histology

Changes in the liver architecture in response to GNPs and I3C treatments were assessed by H&E staining of liver sections. The data are presented in Fig. 3. Liver tissue of rats exposed to GNPs, demonstrated a marked congestion of central vein, vacuolization in cytoplasm of hepatocytes and the hepatic necrosis of foci, along with inflammatory cell influx, as compared to normal histology found in the liver tissue of control rats. On the other hand, these GNP-induced changes, were significantly reversed in rats co-treated with GNPs and I3C, as evident from reduced congestion and fewer inflammatory cell

Table 2 The levels of oxidative stress markers in liver tissues of control and treated rats.

Parameters	G1 (control)	G2 (AuNP)	G3 (I3C)	G4 (AuNP + I3C)
MDA (nmol/mg protein)	1.03 ± 0.04	1.9 ± 0.19[a]	1.02 ± 0.07[a]	1.39 ± 0.05[b]
8-OHdG (nmol/mg protein)	0.17 ± 0.005	0.35 ± 0.007[a]	0.18 ± 0.008[a]	0.22 ± 0.005[b]
GST (nmol/min/mg protein)	13.1 ± 1.19	5.9 ± 0.73[a]	10.3 ± 0.93[a]	10.81 ± 0.73[b]
GR (nmol/min/mg protein)	59.3 ± 4.4	33.8 ± 3.01[a]	55.0 ± 2.83[a]	37.7 ± 3.19[b]

MDA, Malondialdehyde; 8-OHdG, 8-hydroxydeoxyguanosine; GST, Glutathione S-transferase; GR, glutathione reductase.[a] Compared to G1 group, and [b]Ccompared to G2, [ab]$p < 0.01$. Data are presented as mean ± S (N = 10).

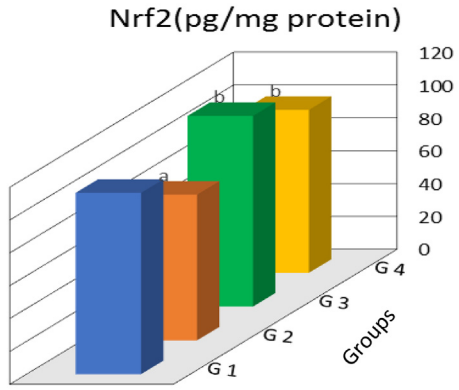

Fig. 2 Nuclear factor erythroid 2-related factor 2 (Nrf2) levels in liver tissues of control and treated rats. G1, control; G2, AuNP treated rats; G3, I3C treated rats; G4, AuNP + I3C treated rats. Data are presented as mean ± SD. [a]Significantly different ($p < 0.01$) compared to G1 group [b]Significantly different ($p < 0.01$) compared to G2 group.

infiltrations. No change in liver histology in rats treated only with I3C was found compared to that of control indicating lack of any apparent effects of I3C alone on liver histology.

3.5. Molecular docking

Auto Dock and MOE tools were used to verify hepatoprotective properties of indole-3-carbinol to support the experimental outcome. Molecular docking with the crystal structure of indole-3-carbinol over liver in which growth factor receptor is highly expressed (Zayed et al., 2018b). Pictorial representation of best possible binding sites of liver protein LT3 (PDB code: 4RT7) with synthesized compounds is shown in Fig. 4. The results of the docking studies show that the compounds interacted favourably with the active binding sites of the proteins in amino acids (4rt7-h/A1/A/ASP‘829/HN–with hydrogen bond length = 2.2 Ao, 4rt7-h/A1/A/VAL‘675/O– with hydrogen bond length = 2.7 Ao and 4rt7-h/A1/A/ILE‘827/O– with hydrogen bond length = 2.8 Ao, the calculated free energy of binding for 1-indole-3-carbinol in the receptor binding site was −6.12 kcal/mol.

4. Discussion

The findings of the present study identify the liver as a primary target organ for GNPs as significant changes in liver functional markers, oxidative stress and inflammatory markers and histopathological changes in liver tissues were noted in GNP treated rats. Further, these adverse effects indicate the possible accumulation GNPs in liver tissue as evident from previous study (Lanone and Boczkowski,2006). Besides, this study

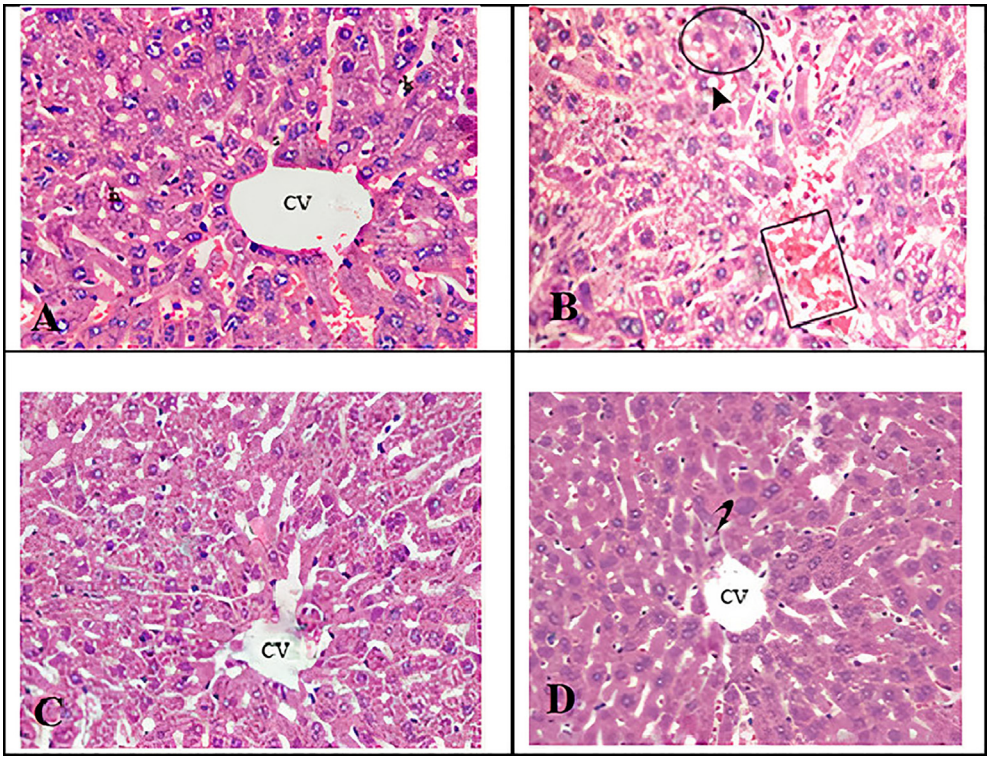

Fig. 3 Micrographs of H&E stained liver sections of rats. (A) Control rats displaying normal histology. (B) Rats exposed to gold NPs exhibiting congestion of the central vein (square), cytoplasmic vacuolisation of hepatocytes (arrow head) and hepatic necrosis of foci along with inflammatory cell influx (circle). (C) Rats exposed to gold NPs and treated with I3C, demonstrating reduced congestion and fewer inflammatory cell population. (D). Rats treated only with I3C showing normal liver architecture. CV; central vein.

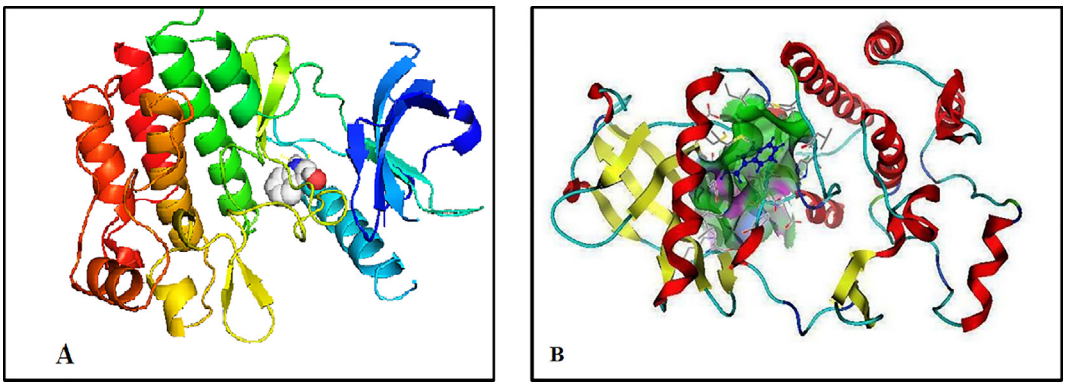

Fig. 4 3D plot interaction of indole-3-carbinol ligand with liver protein LT3 (PDB) code: 4RT7) receptor by Auto dock (A) and MOE (B) methods.

demonstrates the protective effects of I3C in alleviating GNP-induced changes.

4.1. Effect of small sized gold nanoparticles diameter

The GNPs of 10 nm diameter size used in the present study are proven to exert most adverse effects on liver tissue. stated that, Smaller-sized GNPs showed tissue distribution within 3 days after their administration through inhalation, or through oral/dermal exposure, as its absorption and distribution into the blood circulation depended mainly on the size of GNPs (Abdelhalim and Jarrar, 2011). Similarly, the accumulation of GNPs in rat liver 24 h after intravenous injection, was found to be in the range of 91.9 to 96.9% for 200, 80, 10 and 5 nm sizes (Hirn et al., 2011). Whereas, the hepatobiliary clearance of GNPs (from liver to small intestine to fecal excretion) showed an inverse linear relationship for GNPs with size range of 5 nm to 200 nm. Niidome et al. (2006) showed that GNPs with 65 ± 5 nm size were accumulated in liver

It is proposed that liver was the main target of GNPs as they were shown to be accumulated in the liver within minutes after their injection. Additionally a significant fraction of 18 nm sized GNPs are eliminated from blood and accumulated mainly in the spleen and liver. Collectively, above data suggest that smaller sized GNPs accumulate rapidly and in large amounts in liver and that the liver is the primary organ of their accumulation.

4.2. Effects of GNPs and I3C on liver function

The present data showed that, GNPs significantly impaired liver function as all the studied liver functional parameters including ALT, AST, ALP, and total bilirubin and direct bilirubin significantly increased, while albumin level significantly decreased in response to GNPs. Serum AST and ALT levels are indicators of liver injury: as their levels increase as a result of hepatotoxicity, hepatitis or hepatic cirrhosis. The increased activities of these enzymes also related to structural changes in liver damage, which corroborates with greater membrane permeability resulting in an increased leaking of these enzyme into circulation (Sheth et al., 1998).

The findings of adverse effects of GNPs on liver function are consistent with previous studies which have reported similar cytotoxic effects induced by GNPs under both *in vivo* and *in vitro* conditions (Ali et al., 2020; BarathManiKanth et al., 2010). Importantly, different levels of toxic effects have been observed depending on the particle size, shape, dose, sampling points, surface coating and functionalization of GNPs (Tao 2018), Besides, differences in cell lines or animal models have also been contributed to different levels cytotoxic effects of GNPs (Tao 2018). The main toxicity mechanism of GNPs includes cell damage via extrinsic and intrinsic apoptotic pathways (Huo et al., 2018). Additionally, the cytotoxic effects of GNPs also depend on their cellular uptake rate, cell phenotype, internalisation, kinetics of dissociation and its comparative location inside microarchitecture of liver (Tsoi et al., 2016).

In the present study, a significant reversal in all the tested functional markers of liver was noticed in rats co-treated with GNPs and I3C demonstrating the protective effects of I3C against GNP induced functional impairment of liver functions. The favourable effects of I3C found in this study are in agreement with previous studies. (Hasan et al., 2018) The I3C exhibited hepatoprotective effects against several carcinogens, including diethylnitrosamine, 2-acetylaminofluorine and trabectedin, and prevented the development of hepatic cancer in an animal model (Hasan et al., 2018). Likewise, I3C attenuated the aflatoxin B induced hepatic cancer (Dalessandri et al., 2004).

4.3. Effect of GNPs and I3C on oxidative biomarkers in liver tissue

Oxidative stress results due to an imbalance in the levels of oxidants and antioxidants wherein the generation of reactive oxygen species (ROS) over takes the antioxidant levels leading to cellular damage. In the present study rats treated with GNPs showed significantly increased oxidative stress marker MDA, 8-OHdG and significantly decreases antioxidants including GST and GR in liver tissue. Thus the imbalance of oxidants to antioxidant levels confirms the oxidative status conditions in the liver of rats treated with GNPs and thereby further confirms the capacity of GNPs to induce oxidative stress. Oxidative stress inducing power of GNPs has been demonstrated by earlier studies, corroborating with the finding in this study. Oxidative stress, apoptosis and DNA damage were found to be major pathological conditions observed in rats treated with GNPs (Lu et al., 2009; Yu et al., 2007, Lankoff et al., 2012).

In addition, nanoparticles of metallic nature as well as the presence of transitional metals have shown to generate ROS and subsequent oxidative damage (Kovács et al., 2016). Similarly, GNPs were shown to directly affect membrane integrity by structurally an functionally altering intra- and extracellular biomolecules by generating oxidative stress (Boisselier and Astruc, 2009). The 8-OHdG is a well-established marker for oxidative stress induced DNA damage. Its levels were increased in GNP treated rats in the present study suggesting possible DNA damaging effects due to oxidative stress induced by GNPs. Similar observations were made where GNPs were shown to increase 8-OHdG levels and negatively affect the genes associated with genome stability and DNA repair (Li et al., 2018). The GST and GR are antioxidants whose reduced levels tilt the balance towards oxidative stress (Kamat, 2002). As found in the present study, a reduction of GST and GR was noted in liver tissues of rats exposed to GNPs underscoring the increased oxidative stress due to depletion of antioxidants (Al-Hamadani et al., 2020) Nrf2 is a transcription factor which transactivates an array of antioxidant genes as a defensive mechanism to counter oxidative stress. In the present study there was decrease in Nrf2 levels, which may be attributed to either its translocation from cytosol to nucleus or its possibly reduced expression in response to GNPs.

The data in the current study demonstrated antioxidant potential of I3C as all the studied markers including MDA, GST, GR and 8-OHdG were restored to their normal levels in rats co-treated with GNPs and I3C. In line with these observations reports have shown antioxidant potential of I3C. In animal models I3C effectively diminished experimentally induced oxidative stress and reduced the risk of developing lung, colon, liver and breast cancers (El-Naga et al., 2014; Andreadou et al., 2002). The I3C has been shown to attenuate hyperglycaemia induced oxidative stress and protect from neurotoxicity in mice (Jayakumar et al., 2014). Additionally, breast cancer cells treated with I3C upregulated GST and abrogated lipid peroxidation underscoring its antioxidant potential (Szaefer et al., 2015; Lai et al., 2015). In the present study, I3C treatment also restored cytosolic Nrf2 levels, which could be attributed to its increased expression in response to I3C.

The favourable effects of I3C on liver function achieved through intraperitoneal administration diverges from previous studies which have indicated that the beneficial effects of I3C are achieved only if administered orally as it is converted to its acid condensation products in the gastric juices of stomach (Grose and Bjeldanes, 1992, Anderton et al., 2004).‘

4.4. Effect of GNPs and I3C on IL-6

The increased IL-6 levels in rats treated with GNPs points to existence of inflammatory conditions and indicate proinflammatory nature of GNPs. Consistent with this observation, previous studies found GNPs to upregulate IL-6 production and secretion (Bailly et al., 2019) Whereas other studies suggest that the response to inflammation is quickly normalised after an acute phase of treatment (Khan et al., 2013). Importantly, larger sized GNPs (60 nm) were unable to elicit proinflammatory responses (IL-6) in murine macrophages despite their cellular uptake and localization within intracellular vacuoles. Although the relationship between oxidative stress and inflammation has been published in many reports, its function on inflammatory diseases is still uncertain (Leonavičienė et al., 2012).

Decreased IL-6 levels in response to I3C treatment underscore its antiinflammatory properties. This action of I3C may be its direct effect on downregulating IL-6 production or an indirect effect achieved as a result of subsided oxidative stress. Corroborating with this observation, I3C has been shown as a powerful anti-inflammatory agent in rat models of inflammatory diseases due to its capacity to block inflammatory cell infiltration including IL-6 (El-Naga et al., 2014). Likewise, I3C inhibited LPS-induced inflammatory response by blocking TRIF-dependent signaling pathway in macrophages (Jiang et al., 2013) which suggested that, I3C may provide a valuable therapeutic strategy in treating various inflammatory diseases. Furthermore, I3C was proved to ameliorate colonic inflammation (Alkarkoushi et al.,(2019).

4.5. Effect of GNPs and I3C on liver histology

Histological data showed that rats treated with GNPs demonstrated marked pathological changes in liver histology. This correlates well with the impaired liver function observed in GNP treated rats. In line with present data, GNPs have reported to induce hepatocyte injury, adema and cytoplasm vacuolation, indicating subacute and acute liver damage (Abdelhalim and Jarrar, 2011, Abdelhalim and Jarrar, 2012). I3C treatment significantly reversed the GNP induced changes in liver histology, substantiating the protective effects of I3C.

4.6. Molecular docking studies substantiate the experimental data

Auto Dock and MOE tools were used to verify hepatoprotective effects of indole-3-carbinol and to support the experimental actual experimental data. Molecular docking with the crystal structure of indole-3-carbinol over liver in which growth factor receptor is highly expressed showed the best possible binding sites of LT3 with synthesized compounds and that the compounds interacted favourably with the active binding sites. Above findings clearly confirm the obtained experimental data and substantiates the favourable effects of I3C against GNP induced hepatotoxicity.

5. Conclusion

This study demonstrated that GNPs significantly impaired liver function as evident from increased levels of liver functional markers as well as histopathological changes found in rats treated with GNPs. These adverse reactions appear to be mediated by oxidative stress and inflammation as all the studied markers of these pathophysiological conditions are dysregulated in GNP treated rats. The other major finding of the study is the protective effects of I3C against GNP induced changes in liver function and architecture. These favourable effects of I3C can be attributed to the capacity of I3C to blunt oxidative stress and inflammation. Additionally, molecular docking data supported the experimental findings thereby, substantiating the protective effects of I3C against GNP induced hepatotoxicity. Thus, regular consumption of plant based diet rich in I3C may impart beneficial health effects.

Funding

No funding received from public, commercial, or not-for-profit funding agencies for this study.

Declaration of Competing Interest

The authors declare that they have no known competing financial interests or personal relationships that could have appeared to influence the work reported in this paper.

References

Abdelhalim, M., Jarrar, B.M., 2011. Gold nanoparticles administration induced prominent inflammatory, central vein intima disruption, fatty change and Kupffer cells hyperplasia. Lipids Health Dis. 10 (1), 133. https://doi.org/10.1186/1476-511X-10-133.

Abdelhalim, M., Jarrar, B.M., 2012. Histological alterations in the liver of rats induced by different gold nanoparticle sizes, doses and exposure duration. J. Nanobiotechnol. 10 (1), 5. https://doi.org/10.1186/1477-3155-10-5.

Abdelhalim, M.A., Moussa, S.A., 2013. The gold nanoparticle size and exposure duration effect on the liver and kidney function of rats: In vivo. Saudi J. Biol. Sci. 20 (2), 177–181. https://doi.org/10.1016/j.sjbs.2013.01.007.

Adewale, O.B., Davids, H., Cairncross, L., Roux, S., 2019. Toxicological behavior of gold nanoparticles on various models: influence of physicochemical properties and other factors. Int. J. Toxicol. 38 (5), 357–384.

Ali, A., Ovais, M., Cui, X., Rui, Y., Chen, C., 2020. Safety assessment of nanomaterials for antimicrobial applications. Chem. Res. Toxicol. 33 (5), 1082–1109.

Alkarkoushi, R.R., Singh, U.P., Chatzistamou, I., Bam, M., Hui, Y., Nagarkatti, M., Nagarkatti, P., Testerman, T.L., 2019. Indole-3-carbinol ameliorates colonic inflammation in DSS-treated, Helicobacter muridarum-infected mice. J. Immunol. 202, 185.4.

Anderton, M.J., Manson, M.M., Verschoyle, R.D., Gescher, A., Lamb, J.H., Farmer, P.B., Steward, W.P., Williams, M.L., 2004. Pharmacokinetics and tissue disposition of indole-3-carbinol and its acid condensation products after oral administration to mice. Clin. Cancer Res. 10 (15), 5233–5241. https://doi.org/10.1158/1078-0432.CCR-04-0163.

Andreadou, I., Tasouli ,A., Bofilis, E., Chrysselis, M., Rekka, E., Tsantili-Kakoulidou, A., Iliodromitis, E., Siatra, T., Kremastinos, D.T., 2002. Antioxidant activity of novel indole derivatives and protection of the myocardial damage in rabbits. Chem. Pharmaceut. Bull. 50(2), 165–168. https://doi.org/10.1248/cpb.50.16.

Bailly, A.-L., Correard, F., Popov, A., Tselikov, G., Chaspoul, F., Appay, R., Al-Kattan, A., Kabashin, A.V., Braguer, D., Esteve, M.-A., 2019. In vivo evaluation of safety, biodistribution and pharmacokinetics of laser-synthesized gold nanoparticles. Sci Rep 9 (1). https://doi.org/10.1038/s41598-019-48748-3.

BarathManiKanth, S., Kalishwaralal, K., Sriram, M., Pandian, SureshBabu, Youn, H.-S., Eom, SooHyun, Gurunathan, S., 2010. Anti-oxidant effect of gold nanoparticles restrains hyperglycemic conditions in diabetic mice. J. Nanobiotechnol. 8 (1), 16. https://doi.org/10.1186/1477-3155-8-16.

Boisselier, E., Astruc, D., 2009. Gold nanoparticles in nanomedicine: preparations, imaging, diagnostics, therapies and toxicity. Chem. Soc. Rev. 38 (6), 1759–1782. https://doi.org/10.1039/b806051g.

Cross, J.B., Thompson, D.C., Rai, B.K., Baber, J.C., Fan, K.Y., Hu, Y., Humblet, C., 2009. Comparison of several molecular docking programs: pose prediction and virtual screening accuracy. J. Chem. Inf. Model. 49 (6), 1455–1474.

Dalessandri, K.M., Firestone, G.L., Fitch, M.D., Bradlow, H.L., Bjeldanes, L.F., 2004. Pilot Study: Effect of 3,3′-Diindolylmethane Supplements on Urinary Hormone Metabolites in Postmenopausal Women With a History of Early-Stage Breast Cancer. Nutr. Cancer 50 (2), 161–167.

Dobbs, K.D., Hehre, W.J., 1987. Molecular orbital theory of the properties of inorganic and organometallic compounds. 6. Extended basis sets for second-row transition metals. J. Comput. Chem. 8 (6), 880–893.

Draper, H.H., Hadley, M., 1990. Melondialdehyde determination as an index of lipid peroxidation. Methods Enzymol. 186, 421–425.

El-Naga, R.N., Ahmed, H.I., Abd Al Haleem, E.N., 2014. Effects of indole-3-carbinol on clonidine-induced neurotoxicity in rats: impact on oxidative stress, inflammation, apoptosis and monoamine levels. Neurotoxicology 44: 48–57 doi: docking10.1016/j.neuro.2014.05.004.

Grose, Karl R., Bjeldanes, Leonard F., 1992. Oligomerization of indole-3-carbinol in aqueous acid. Chem. Res. Toxicol. 5 (2), 188–193.

Hasan, H., Ismail, H., El-Orfali, Y., Khawaja, G., 2018. Therapeutic benefits of Indole-3-Carbinol in adjuvant-induced arthritis and its protective effect against methotrexate induced-hepatic toxicity. BMC Complement. Alternative Med. 18 (1), 337.

Hirn, S., Semmler-Behnke, M., Schleh, C., Wenk, A., Lipka, J., Schäffler, M., Takenaka, S., Möller, W., Schmid, G., Simon, U., Kreyling, W.G., 2011. Particle size-dependent and surface charge-dependent biodistribution of gold nanoparticles after intravenous administration. Eur. J. Pharm. Biopharm. 77 (3), 407–416.

Huang, L., Liu, M., Huang, H., Wen, Y., Zhang, X., Wei, Y., 2018. Recent advances and progress on melanin-like materials and their biomedical applications. Biomacromolecules 19 (6), 1858–1868.

Huo, Yue, Singh, Priyanka, Kim, Yeon Ju, Soshnikova, Veronika, Kang, Jongpyo, Markus, Josua, Ahn, Sungeun, Castro-Aceituno, Verónica, Mathiyalagan, Ramya, Chokkalingam, Mohan, Bae, Kwi-Sik, Yang, Deok Chun, 2018. Biological synthesis of gold and silver chloride nanoparticles by Glycyrrhiza uralensis and in vitro applications. Artif. Cells Nanomed. Biotechnol. 46 (2), 303–312.

Jayakumar, Poornima, Pugalendi, Kodukkur Vishwanath, Sankaran, Mirunalini, 2014. Attenuation of hyperglycemia-mediated oxidative stress by indole-3-carbinol and its metabolite 3, 3′- diindolylmethane in C57BL/6J mice. J Physiol Biochem 70 (2), 525–534.

Jiang, J., Kang, T.B., Oh, N.H., Kim, T.J., Lee, K.H., 2013. Indole-3-carbinol inhibits LPS-induced inflammatory response by blocking TRIF-dependent signaling pathway in macrophages. Food Chem. Toxicol. 57, 256–261.

Kamat, P.V., 2002. Photophysical, photochemical and photocatalytic aspects of metal nanoparticles. J. Phys. Chem. B. 106, 7729–7744.

Katz, Ella, Nisani, Sophia, Yadav, Brijesh S., Woldemariam, Melkamu G., Shai, Ben, Obolski, Uri, Ehrlich, Marcelo, Shani, Eilon, Jander, Georg, Chamovitz, Daniel A., 2015. The glucosinolate breakdown product indole-3-carbinol acts as an auxin antagonist in roots of Arabidopsis thaliana. Plant J 82 (4), 547–555.

Kim, J.K., Park, S.U., 2018. Current results on the biological and pharmacological activities of Indole-3-carbinol. EXCLI J. 17, 181.

Khan, Haseeb A., Abdelhalim, Mohamed Anwar K., Alhomida, Abdullah S., Al-Ayed, Mohammed S., 2013. Effects of naked gold nanoparticles on proinflammatory cytokines mRNA expression in rat liver and kidney. Biomed Res. Int. 2013, 1–6.

Kovács, Dávid, Igaz, Nóra, Keskeny, Csilla, Bélteky, Péter, Tóth, Tímea, Gáspár, Renáta, Madarász, Dániel, Rázga, Zsolt, Kónya, Zoltán, Boros, Imre M., Kiricsi, Mónika, 2016. Silver nanoparticles defeat p53-positive and p53-negative osteosarcoma cells by triggering mitochondrial stress and apoptosis. Sci. Rep. 6 (1). https://doi.org/10.1038/srep27902.

Lai, T.H., Shieh, J.M., Tsou, C.J., Wu, W.B., 2015. Gold nanoparticles induce heme oxygenase-1 expression through Nrf2 activation and Bach1 export in human vascular endothelial cells. Int. J. Nanomed. 10, 5925. https://doi.org/10.2147/IJN.S88514.

Lankoff, A., Sandberg, W.J., Wegierek-Ciuk, A., Lisowska, H., Refsnes, M., Sartowska, B., Schwarze, P.E., Meczynska-Wielgosz,

S., Wojewodzka, M., Kruszewski, M., 2012. The effect of agglomeration state of silver and titanium dioxide nanoparticles on cellular response of HepG2, A549 and THP-1 cells. Toxicol. Lett. 208(3), 197–213 (5) doi:10.1016/j.toxlet.2011.11.00.

Lanone, S., Boczkowski, J., 2006. Biomedical applications and potential health risks of nanomaterials: molecular mechanisms. Curr. Mol. Med. 1;6(6):651-63 (2006).

Leibelt, D.A., Hedstrom, O.R., Fischer, K.A., Pereira, C.B., Williams, D.E., 2003. Evaluation of chronic dietary exposure to indole-3-carbinol and absorption-enhanced 3, 3′-diindolylmethane in sprague-dawley rats. Toxicol. Sci. 74 (1), 10–21.

Leonavičienė, L., Kirdaitė, G., Bradūnaitė, R., Vaitkienė, D., Vasiliauskas, A., Zabulytė, D., Ramanavičienė, A., Ramanavičius, A., Ašmenavičius, T., Mackiewicz, Z., 2012. Effect of gold nanoparticles in the treatment of established collagen arthritis in rats. Medicina. 48 (2), 16. https://doi.org/10.3390/medicina48020016.

Li, X., Li, Y., Cheng, T., Liu, Z., Wang, R., 2010. Evaluation of the performance of four molecular docking programs on a diverse set of protein-ligand complexes. J. Comput. Chem. 31 (11), 2109–2125.

Li, Taotao, Yi, Huan, Liu, Yuan, Wang, Zunliang, Liu, Shiquan, He, Nongyue, Liu, Hongna, Deng, Yan, 2018. One-Step Synthesis of DNA Templated Water-Soluble Au–Ag Bimetallic Nanoclusters for Ratiometric Fluorescence Detection of DNA. j biomed nanotechnol 14 (1), 150–160.

Lu, Senlin, Duffin, Rodger, Poland, Craig, Daly, Paul, Murphy, Fiona, Drost, Ellen, MacNee, William, Stone, Vicki, Donaldson, Ken, 2009. Efficacy of Simple Short-Term in Vitro Assays for Predicting the Potential of Metal Oxide Nanoparticles to Cause Pulmonary Inflammation. Environ. Health Perspect. 117 (2), 241–247.

McConkey, B.J., Sobolev, V., Edelman, M., 2002. The performance of current methods in ligand-protein docking. Curr. Sci. 83, 845–855.

Nel, A., Xia, T., Mädler, L., Li, N., 2006. Toxic Potential of Materials at the Nanolevel. Science 311, 622–627. https://doi.org/10.1126/science.

Niidome, Takuro, Yamagata, Masato, Okamoto, Yuri, Akiyama, Yasuyuki, Takahashi, Hironobu, Kawano, Takahito, Katayama, Yoshiki, Niidome, Yasuro, 2006. PEG-modified gold nanorods with a stealth character for in vivo applications. J. Control. Release 114 (3), 343–347.

Oberdörster, G., Maynard, A., Donaldson, K., Castranova, V., Fitzpatrick, J., Ausman, K., Carter, J., Kan, B., Kreyling, W., Lai, D., Olin, S., Monteiro-Riviere, N., Warheit, D., 2005. Principles for characterizing the potential human healtheffects from exposure to nanomaterials: elements of a screening strategy. Part. Fibre Toxicol. 2, 13–35.

Okulicz, M., Hertig, I., Chichlowska, J., 2009. Effects of indole-3-carbinol on metabolic parameters and on lipogenesis and lipolysis in adipocytes. Czech J. Anim. Sci. 54 (4), 182. https://doi.org/10.17221/1745-CJAS.

Plewczynski, Dariusz, Łaźniewski, Michał, Augustyniak, Rafał, Ginalski, Krzysztof, 2011. Can we trust docking results? Evaluation of seven commonly used programs on PDBbind database. J. Comput. Chem. 32 (4), 742–755.

Reed, G.A., Arneson, D.W., Putnam, W.C., Smith, H.J., Gray, J.C., Sullivan, D.K., Mayo, M.S., Crowell, J.A., Hurwitz, A., 2006. Single-Dose and Multiple-Dose Administration of Indole-3-Carbinol to Women: Pharmacokinetics Based on 3,3'-Diindolylmethane. Cancer Epidemiol. Biomark. Prev. 15 (12), 2477–2481. https://doi.org/10.1158/1055-9965.EPI-06-0396.

Sheth, Sunil G, Flamm, Steven L, Gordon, Fredric D, Chopra, Sanjiv, 1998. AST/ALT Ratio Predicts Cirrhosis in Patients With Chronic Hepatitis C Virus Infection:. Am. J. Gastroenterol. 93 (1), 44–48.

Shu, J., Tang, D., 2019. Recent advances in photoelectrochemical sensing: from engineered photoactive materials to sensing devices and detection modes. Anal. Chem. 92 (1), 363–377.

Siddiqi, N.J., Abdelhalim, M.A., El-Ansary, A.K., Alhomida, A.S., Ong, W.Y., 2012. Identification of potential biomarkers of gold nanoparticle toxicity in rat brains. Journal of neuroinflammation. 9 (1), 123. https://doi.org/10.1186/1742-2094-9-123.

Sung, J.H., et al., 2012. Subacute oral toxicity investigation of nanoparticulate and ionic silver in rats. Arch. Toxicol. 86, 543–551 doi:10.1007/s00204-011-0759-1.

Szaefer, Hanna, Krajka-Kuźniak, Violetta, Licznerska, Barbara, Bartoszek, Agnieszka, Baer-Dubowska, Wanda, 2015. Cabbage Juices and Indoles Modulate the Expression Profile of AhR, ERα, and Nrf2 in Human Breast Cell Lines. Nutr. Cancer 67 (8), 1344–1356.

Tao, C., 2018. Antimicrobial activity and toxicity of gold nanoparticles: research progress, challenges and prospects. Lett. Appl. Microbiol. 67(6), 537-543.(2018).

Al-Hamadani, M.Y.I., Alzahrani, A.M., Yousef, M.I., Kamel, M.A., El-Sayed, W.M., 2020. Gold Nanoparticles Perturb Drug-Metabolizing Enzymes and Antioxidants in the Livers of Male Rats: Potential Impact on Drug Interactions. Int J Nanomedicine. 14 (15), 5005–5016.

Tsoi, K.M., MacParland, S.A., Ma, X.Z., Spetzler, V.N., Echeverri, J., Ouyang, B., Fadel, S.M., Sykes, E.A., Goldaracena, N., Kaths, J. M., Conneely, J.B., 2016. Mechanism of hard-nanomaterial clearance by the liver. Nat. Mater. 15 (11), 1212. https://doi.org/10.1038/nmat4718.

Xue, Yuying, Zhang, Shanshan, Huang, Yanmei, Zhang, Ting, Liu, Xiaorun, Hu, Yuanyuan, Zhang, Zhiyong, Tang, Meng, 2012. Acute toxic effects and gender-related biokinetics of silver nanoparticles following an intravenous injection in mice: Acute toxic effects and gender-related biokinetics of AgNPs in mice. J. Appl. Toxicol. 32 (11), 890–899.

Yu, L.E., Lanry, Yung. L.Y., Ong, C.N., Tan, Y.L., Suresh Balasubramaniam K, Hartono, D., Shui, G., Wenk, M.R., Ong, W.Y., 2007. Translocation and effects of gold nanoparticles after inhalation exposure in rats. Nanotoxicology 1(3): 235–242. (2007) doi: 10.1016/j.taap.2016.02.004

Zayed, Ehab M., Hindy, Ahmed M.M., Mohamed, Gehad G., 2018a. Molecular structure, molecular docking, thermal, spectroscopic and biological activity studies of bis-Schiff base ligand and its metal complexes. Appl Organometal Chem 32 (1), e3952. https://doi.org/10.1002/aoc.3952.

Zayed, Ehab M., Zayed, Mohamed A., Abd El Salam, Hayam A., Nawwar, Galal A.M., 2018b. Synthesis, structural characterization, density functional theory (B3LYP) calculations, thermal behaviour, docking and antimicrobial activity of 4-amino-5-(heptadec-8-en-1-yl)-4 H -1,2,4-triazole-3-thiol and its metal chelates : Synthesis, Structure of Triazole ligand its chelates and MOCs,. Appl Organometal Chem 32 (12), e4535. https://doi.org/10.1002/aoc.v32.1210.1002/aoc.4535.

Zayed, Ehab M., Zayed, M.A., Abd El Salam, Hayam A., Noamaan, Mahmoud A., 2019. Novel Triazole Thiole ligand and some of its metal chelates: Synthesis, structure charactertization, thermal behavior in comparison withcomputational caculations andbiological activities. Comput. Biol. Chem. 78, 260–272.